

Flexible, Mechanically Stable, Porous Self-Standing Microfiber Network Membranes of Covalent Organic Frameworks: Preparation Method and Characterization

Chenhui Ding, Marion Breunig, Jana Timm, Roland Marschall, Jürgen Senker,* and Seema Agarwal*

Covalent organic frameworks (COFs) show advantageous characteristics, such as an ordered pore structure and a large surface area for gas storage and separation, energy storage, catalysis, and molecular separation. However, COFs usually exist as difficult-to-process powders, and preparing continuous, robust, flexible, foldable, and rollable COF membranes is still a challenge. Herein, such COF membranes with fiber morphology for the first time prepared via a newly introduced template-assisted framework process are reported. This method uses electrospun porous polymer membranes as a sacrificial large dimension template for making self-standing COF membranes. The porous COF fiber membranes, besides having high crystallinity, also show a large surface area ($1153 \text{ m}^2 \text{ g}^{-1}$), good mechanical stability, excellent thermal stability, and flexibility. This study opens up the possibility of preparation of large dimension COF membranes and their derivatives in a simple way and hence shows promise in technical applications in separation, catalysis, and energy in the future.

bonds in the form of a 2D or 3D structure.^[1] Their controllable crystalline structure, high chemical and thermal stability, and permanent porosity with high specific surface areas have made them promising for a wide range of applications in fields, including gas storage,^[2] separation,^[3] catalysis,^[4] water purification,^[5] molecular separations,^[6] energy storage,^[7] and light-emitting diodes.^[8] Despite several advantages and suitability for various application areas, the actual use is limited due to their nonprocessability originating from the cross-linked insoluble and infusible structure.^[9] To solve this problem, researchers have adopted various methods to obtain COFs with different morphologies, including hollow tubes,^[10] core-shell structures,^[11] membranes,^[12] and foams.^[13]

Recently, some research efforts were invested in preparing COF membranes

1. Introduction

Covalent organic frameworks (COFs) are crystalline porous macromolecular networks linked through strong covalent

which can be categorized into four types. The first is to grow the COF composite membranes directly on the supporting carrier in situ, but this requires a supporting carrier, and there is a problem of adhesion.^[14] The second method is to obtain COF nanosheets by mechanical grinding or chemical treatment, but the weak interaction force between COF nanosheets usually leads to poor mechanical properties of the assembled COF films.^[15] The third method is to prepare COF membranes through liquid-liquid interface polymerization, but the COF membranes have poor mechanical properties and low crystallinity.^[16] The fourth method is to obtain the COF membranes by baking the organic linking agent with the corresponding aldehydes, but the thickness of the COF membranes is several hundred microns.^[9] Therefore, there is an urgent need for new preparation methods for self-standing COF membranes with large dimensions, excellent crystallinity, and mechanical properties. Without large dimension processable self-standing flexible COF membranes, their applications are limited.

We set this as our goal and report the preparation of porous, crystalline COF membranes of large dimensions and mechanical stability in a new three-step easy to perform synthesis, which we refer to in the following as template-assisted framework (TAF) process. The method utilizes electrospun porous polymer membranes as a sacrificial large dimension template. Electrospinning is the simplest and most effective method to prepare continuous polymer nanofibers and the corresponding porous membranes of large dimensions, large specific

C. Ding, S. Agarwal
Macromolecular Chemistry and Bavarian Polymer Institute
University of Bayreuth
Universitätsstrasse 30, 95440 Bayreuth, Germany
E-mail: agarwal@uni-bayreuth.de

M. Breunig, J. Senker
Department of Chemistry
Inorganic Chemistry III and Northern Bavarian NMR Centre (NBNC)
University of Bayreuth
Universitätsstrasse 30, 95440 Bayreuth, Germany
E-mail: juergen.senker@uni-bayreuth.de

J. Timm, R. Marschall
Department of Chemistry
Physical Chemistry III
University of Bayreuth
Universitätsstrasse 30, 95440 Bayreuth, Germany

 The ORCID identification number(s) for the author(s) of this article can be found under <https://doi.org/10.1002/adfm.202106507>.

© 2021 The Authors. Advanced Functional Materials published by Wiley-VCH GmbH. This is an open access article under the terms of the Creative Commons Attribution License, which permits use, distribution and reproduction in any medium, provided the original work is properly cited.

DOI: 10.1002/adfm.202106507

surface areas, large porosity, and high flexibility.^[17] The polymer membranes, electrospun with the help of a template polymer, support the in situ growth of the COF. The subsequent removal of the template polymer leaves behind self-standing crystalline COF membranes with high surface area ($1153 \text{ m}^2 \text{ g}^{-1}$), good mechanical stability (tensile strength of 0.64 MPa and excellent bending stability), and flexibility (the mechanical properties remain unchanged after 10 000 bending tests).

2. Results and Discussions

The TAF process used for the preparation of self-standing porous COF membranes is shown in **Figure 1**.

In the first step of the TAF process, one of the COF reactants, the diamine (p-phenylenediamine (Pa)), was immobilized on an electrospun polyacrylonitrile (PAN) fibrous membrane in different amounts by electrospinning of a solution of PAN and Pa. The resulting PAN/Pa fiber membranes with different loadings of Pa (100% and 200% to the amount of PAN) are called PAN/Pa-100 and PAN/Pa-200, respectively. To explore the in situ growth of the COF within the fibers and the resulting morphology, we performed scanning electron microscope (SEM) characterization (**Figure 2**). **Figure 2a–c** shows the SEM images of PAN, PAN/Pa-100, and PAN/Pa-200 fibrous membranes. The pure PAN fibers have a smooth surface, while the PAN/Pa-100 and PAN/Pa-200 show a rough surface and are covered with a layer of Pa. Pa is expected to mix with PAN in the bulk of the fibers and to deposit on the surface.

Moreover, as the content of Pa in PAN/Pa fibers increases, the fiber diameter increases significantly. The average diameter of the PAN fibers, PAN/Pa-100 fibers, and PAN/Pa-200 fibers are 348 ± 84 , 1312 ± 103 , and 1699 ± 147 nm, respectively. This shows that Pa was successfully doped into PAN fibers. In the second step, the COF was grown in situ on PAN fiber membranes by reaction of immobilized Pa with the 1,3,5-triformylphloroglucinol (Tp) (catalyst: acetic acid, temperature: 120 °C, time: 1 day). The corresponding COFs generated on PAN/Pa-100 and PAN/Pa-200 are called PAN/COF-100 and

PAN/COF-200, respectively. For comparison, the conventional synthesis of COF by mixing Tp and Pa led to spherical particles (**Figure 2d**). **Figure 2e,e',f,f'** shows the surface and cross-section morphologies of PAN/COF-100 and PAN/COF-200 fibers. It can be found that with the reaction of Pa and Tp, TpPa COF nanoparticles grow uniformly on the surface of the PAN fibers. Moreover, the cross-section morphology of PAN/COF fibers shows that TpPa COF nanoparticles also grow in the bulk of the fibers. This shows that during the reaction process, Tp not only reacts with Pa on the fiber surface but also penetrates into the bulk of the fiber and reacts with Pa to generate TpPa COF nanoparticles.

In the third step, the removal of the template polymer PAN from the membranes by solvent extraction provided the self-standing porous TpPa COF membranes, COF-100 and COF-200, respectively. **Figure 2g,g',h,h'** shows the surface and cross-section morphology of COF-100 and COF-200 fibers. Compared with PAN/COF fibers, the surface of the porous COF fibers is basically unchanged, and the fiber morphology remains intact. By observing the cross-sectional morphology, it can be found that the porous COF fibers possess porous core-shell-type structures with varied densities of COF particles in the shell and core. This is because, during the in situ growth of TpPa COFs, the surface of the PAN fiber provides enough Pa and enough growth space to form a dense shell composed of TpPa COF nanoparticles. In the bulk of PAN fiber, TpPa COF nanoparticles are wrapped by PAN during the growth process, which leads to a lack of sufficient growth space. Therefore, after the PAN is removed, leaving a porous core is formed by the accumulation of TpPa COF nanoparticles. In addition, the core-shell structure of porous COF fibers ensures that it has good mechanical stability and high specific surface area, as described in the later section. The optical photographs of membranes are shown in **Figure 2** (bottom).

The Fourier-transform infrared (FT-IR) spectra of the samples are shown in **Figures S1 and S2** in the Supporting Information. The characteristic stretching bands at 3100–3300, 2242, 1574, and 1236 cm^{-1} are attributed to the N–H group of Pa, the C≡N group of the PAN, C=C, and C–N of the TpPa

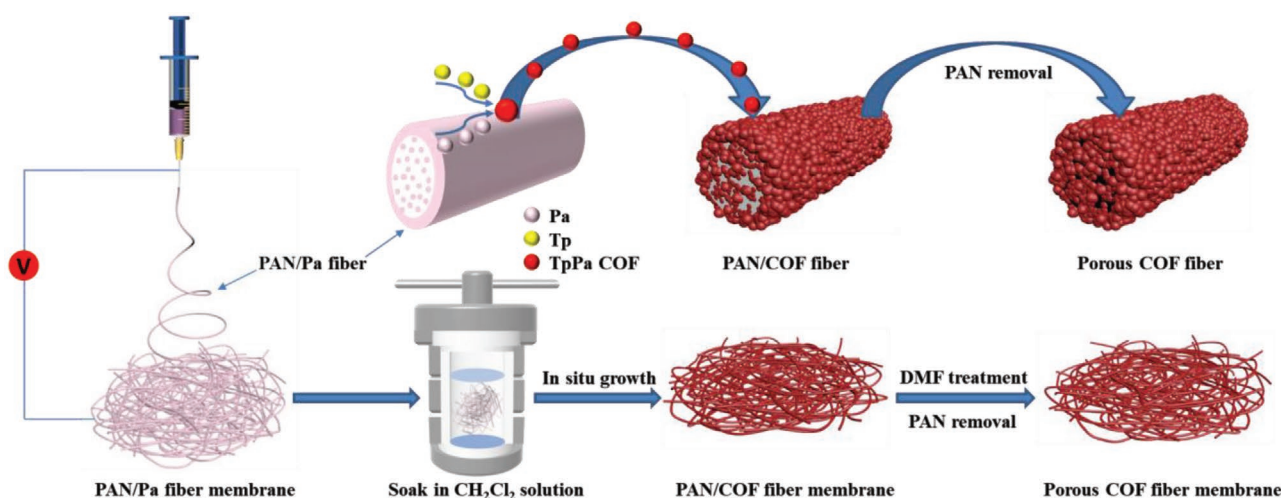


Figure 1. The three-step preparation process of porous COF membranes. PAN = polyacrylonitrile, Pa = p-phenylenediamine, Tp = 1,3,5-triformylphloroglucinol.

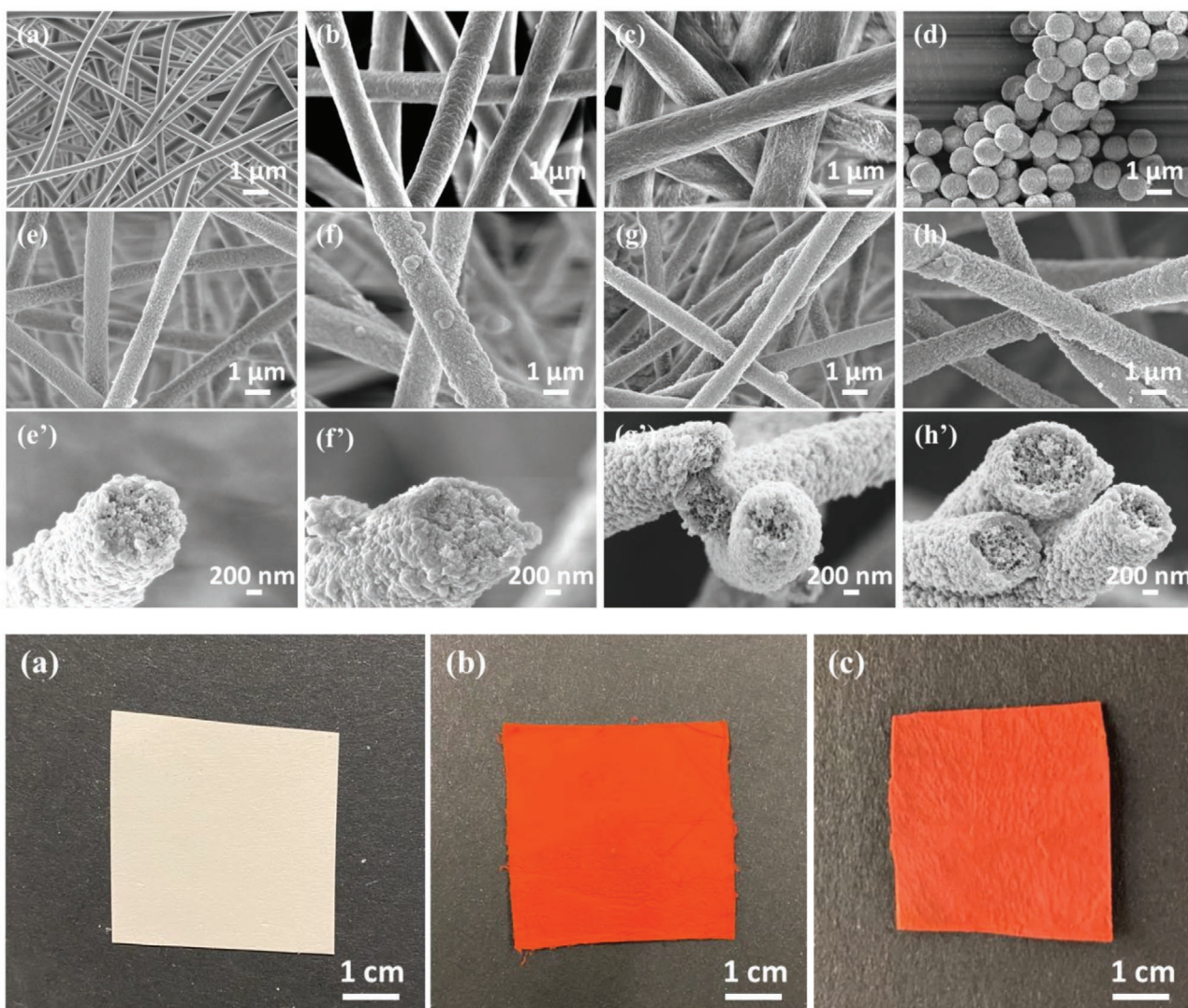


Figure 2. Top: SEM images of a) PAN, b) PAN/Pa-100, c) PAN/Pa-200, d) TpPa COF powder, e) PAN/COF-100, f) PAN/COF-200, g) COF-100, and h) COF-200 with e', f', g', h') their cross-section, respectively. Bottom: Photographs of a) PAN/Pa-100, b) PAN/COF-100, and c) COF-100.

COF, respectively.^[18] In fact, after 1 day of synthesis at 120 °C, the color of PAN/Pa fiber membranes changed from lavender to red. This means that TpPa COF has grown on PAN fibers. It can be found from Figure S1 in the Supporting Information that the characteristic stretching band at 3100–3300 cm^{-1} (N–H) has disappeared, and the characteristic stretching band at 1574 cm^{-1} (C=C) and 1236 cm^{-1} (C–N) is displayed on COF formation. In addition, through the *N,N*-dimethylformamide (DMF) post-treatment for the removal of PAN, the FT-IR spectra of the porous COF fiber membranes and the TpPa COF powders are basically the same. This shows that PAN was effectively removed without changing the chemical structure of TpPa COF, and the porous COF fiber membranes were successfully obtained. The FT-IR spectrum of COF-200 series and Tp are shown in Figure S2 in the Supporting Information.

The ^{13}C (Figure 3a and Figure S3, Supporting Information), as well as ^{15}N (Figure 3b) cross polarized magic angle spinning (CP MAS) NMR spectra, demonstrate for the PAN/Pa-100

fiber mat to be composed of a mixture of PAN and Pa. This is particularly obvious by the characteristic ^{15}N NMR peaks at –127 ppm for the nitrile unit of PAN and at –328 ppm for the amino groups of Pa, as well as by the ^{13}C NMR shifts at around 30 ppm for the aliphatic PAN backbone and at 139 ppm for the aromatic CH groups of Pa. After the reaction of PAN/Pa-100 with Tp, the characteristic peaks for Pa disappear, and resonances typical for COF-100 were observed. Pronounced are shifts at –241 ppm (^{15}N) and 106, 146, and 184 ppm (^{13}C) for the keto-enamine groups arise. The absence of peaks characteristic for amino functions confirms very high cross-linking degrees (>95 %) and thus the success of the polycondensation of the two monomers to COF-100. The remaining PAN peaks demonstrate that PAN/COF-100 represents a composite membrane of PAN and COF-100. PAN could subsequently be removed by Soxhlet extraction, as evident by the disappearance of PAN peaks at –126 ppm (^{15}N) and at 30 and 121 ppm (^{13}C). For the second synthesis series (higher Pa content) similar behavior

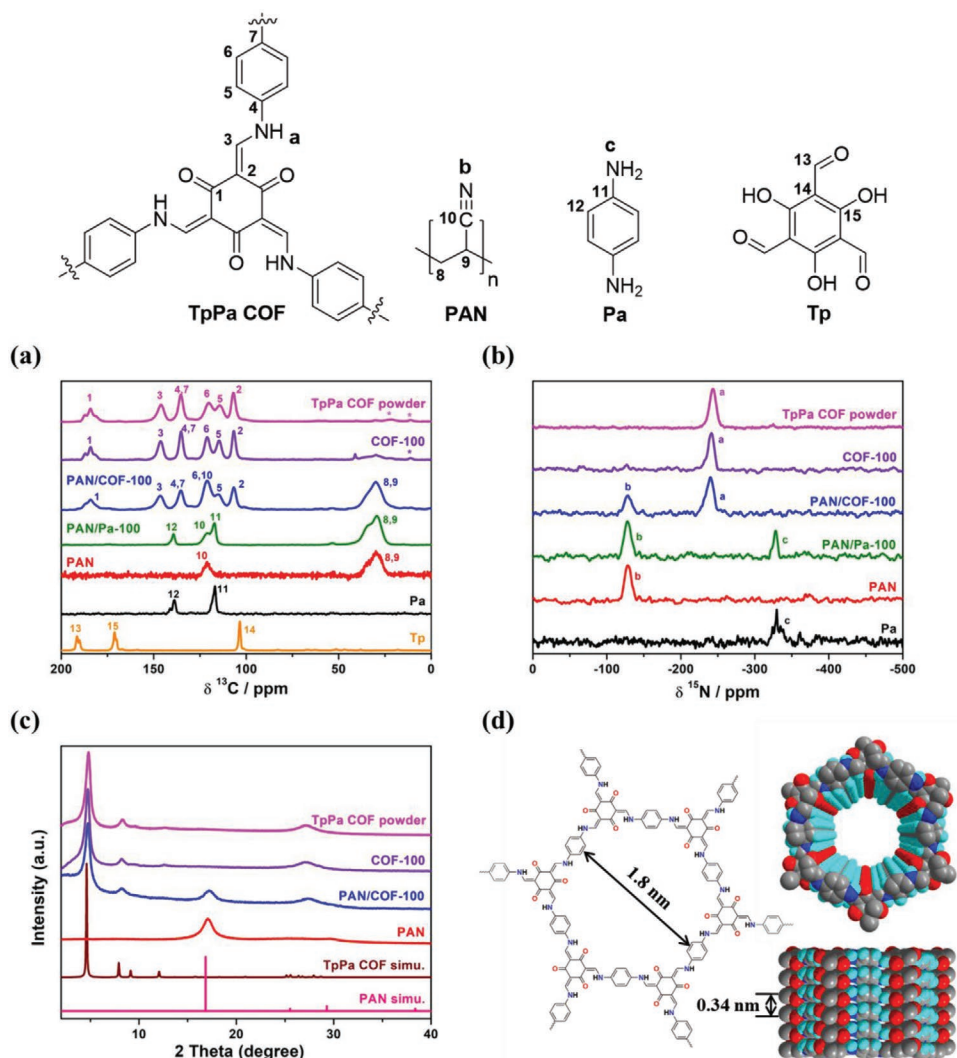


Figure 3. a) ^{13}C and b) ^{15}N CP MAS NMR spectra of the COF-100 series. The asterisks mark spinning sidebands. PXRD patterns of TpPa COF powder (magenta), COF-100 (violet), PAN/COF-100 (blue), and PAN (red). c) The simulated PXRD patterns of TpPa COF (wine) and PAN (pink) are also shown. d) The structure and space-filling model of TpPa COF.

was observed. The data of the COF-200 series are shown in Figure S3 in the Supporting Information.

The X-ray diffraction (XRD) patterns of TpPa COF powder, PAN, PAN/COF, and porous COF fiber membranes are shown in Figure 3c and Figure S4 in the Supporting Information. They show the typical reflexes for the hexagonal metric of TpPa COF^[19] at $2\theta = 4.8^\circ$ (100), 8.5° (210), and 26.9° (001), while the reflex at $2\theta = 17.2^\circ$ is attributed to PAN. According to Bragg's Law, the d spacings of the (100) and (001) reflexes are 1.8 and 0.33 nm, respectively. This is basically consistent with the pore size and eclipse stacking between the layers of TpPa COF reported in the literature.^[19] The XRD data also confirmed that the PAN/COF and porous COF fiber membranes were successfully obtained in this work with a crystallinity comparable to the one of the TpPa COF bulk material.

N_2 and Ar physisorption isotherms were conducted to examine the surface areas, the pore size distributions, and the cumulative pore volumes of TpPa COF powders and material

from different steps of the TAF process (PAN/COF and porous COF fiber membranes). As 2D COFs are sensitive to swelling when exposed in particular to N_2 ,^[20] the pore size distribution and specific surface area of TpPa COF powder were determined using an Ar physisorption isotherm at 87 K (Figure S5, Supporting Information). The isotherm is typical for a microporous material.^[21] The surface area amounts to $463 \text{ m}^2 \text{ g}^{-1}$, the pore size distribution exhibits a maximum at 1.6 nm, and the maximum cumulative pore volume results in $0.2 \text{ cm}^3 \text{ g}^{-1}$, which is in good agreement with the observation from the PXRD patterns and values reported for the traditional solvent synthesis method.^[20] Further gas physisorption measurements of the series PAN/COF and COF fiber membranes were conducted with N_2 at 77 K. Interestingly, only the PAN/COF samples show a slight swelling behavior (adsorption branch and desorption branch not closing at low p/p_0), which derives from the high amount of nonrigid, polymeric material. The absence of swelling for COF-100 and COF-200 indicates that the COF

fiber membranes production creates improved stability against swelling and an additional stiffness compared to the TpPa COF powders. The nitrogen physisorption isotherm of COF-100 is again typical for a microporous material, while the isotherm of COF-200 shows an additional increase at high relative pressures (p/p_0), resulting from voids between the single fibers of COF-200, which might be explained with the larger fiber diameter of COF-200 compared to COF-100.^[21] The pore size distribution of the PAN/COF and COF fiber membranes exhibit maxima between 1.7 and 1.8 nm (Figure 4b), matching the pore sizes of the TpPa COF and the ones determined from the XRD data. An additional micropore diameter of 1.4 nm could be observed for the COF-200 sample. The cumulative pore volumes of COF-100 and COF-200 are more than doubled compared to TpPa COF powder and almost quadrupled compared to PAN/COF. This is because PAN wraps the TpPa COF nanoparticles in the bulk of the PAN fiber, and only the nanoparticles on the fiber's surface are exposed. After PAN removal, the pores are accessible, resulting in a strongly increased pore volume and surface area. The specific surface areas of PAN/COF-100 and PAN/COF-200 are comparable to each other with 229 and 224 $\text{m}^2 \text{g}^{-1}$, respectively, and are much lower than TpPa COF powders. However,

the surface areas of porous COF-100 and porous COF-200 fiber self-standing membranes are much higher and exceed 1120 and 1153 $\text{m}^2 \text{g}^{-1}$, respectively, even the one obtained for the TpPa COF powders. The removal of PAN by solvent extraction creates a hierarchically porous material with a macroporosity (Figure 2) that renders all COF nanoparticles accessible (including in the bulk). Additionally, the TpPa COF particles from the bulk syntheses are larger by one to two orders of magnitude (Figure 2), which makes the latter particles prone to pore blocking. This, in turn, reduces the accessible pore space leading to smaller surface areas for TpPa COF powder compared to COF-100 and COF-200. In particular, the hierarchical build-up of the COF fibers obtained by the TAF process is advantageous for potential applications.

Excellent thermal stability is conducive to expanding the application of TpPa COF. Figure S6 in the Supporting Information shows the thermogravimetric analysis curves of TpPa COF powders, PAN, PAN/COF, and porous COF fiber membranes in a nitrogen atmosphere. $T_{5\%}$ (the temperature at which 5% mass loss takes place) and a residual mass at 800 °C were used to evaluate the thermal stability of the samples, as shown in Table S3 in the Supporting Information. It can be observed that all the samples have good thermal stability, and there is basically no loss before 300 °C. This indicates that PAN/COF and porous COF fiber membranes have potential applications in the high-temperature field. In addition, the residual masses of PAN/COF and porous COF fiber membranes at 800 °C are both greater than 45%, making their carbon derivatives broad application prospects.

Tensile test and cycle test analyze the mechanical properties and flexibility of materials. By changing the content of Pa in the PAN fiber, the mechanical properties of PAN/COF and porous COF fiber membranes were studied, as shown in Figure 5, and the corresponding results are shown in Table S4 in the Supporting Information. The PAN/COF fiber membranes show good mechanical properties, but as the content of Pa increases, the mechanical properties of PAN/COF fiber membranes decrease. This may be due to the fact that more TpPa COF nanoparticles have grown inside the fiber, resulting in more structural defects. In addition, after DMF post-treatment, the PAN is completely removed, and the fibers in COF membranes (COF-100 and COF-200 had thickness around 53 and 59 μm , respectively (Table S4, Supporting Information)) are only composed of TpPa COF nanoparticles. The porous COF-200 fibers may contain more nanoparticles, which results in dense porous COF-200 fiber membranes having better mechanical properties than porous COF-100 fiber membranes. At the same time, the dense TpPa COF nanoparticles shell on the surface of the porous COF fibers ensures its mechanical stability. Few other literature references show the mechanical characteristics of different COF membranes. The membrane prepared in this work shows better mechanical stability than the COF membrane prepared by interfacial polymerization using 1,3,5-triformylbenzene and 2,5-diethoxyterephthalohydrazide as the starting materials (tensile stress 0.26 MPa).^[22] Although mechanical stability of COF membrane in the present work is sufficient for use in several applications, like separation and catalysis, it can be tuned to different values by use of fillers, modified multifunctional polymers as building blocks, etc. The highest tensile strength of

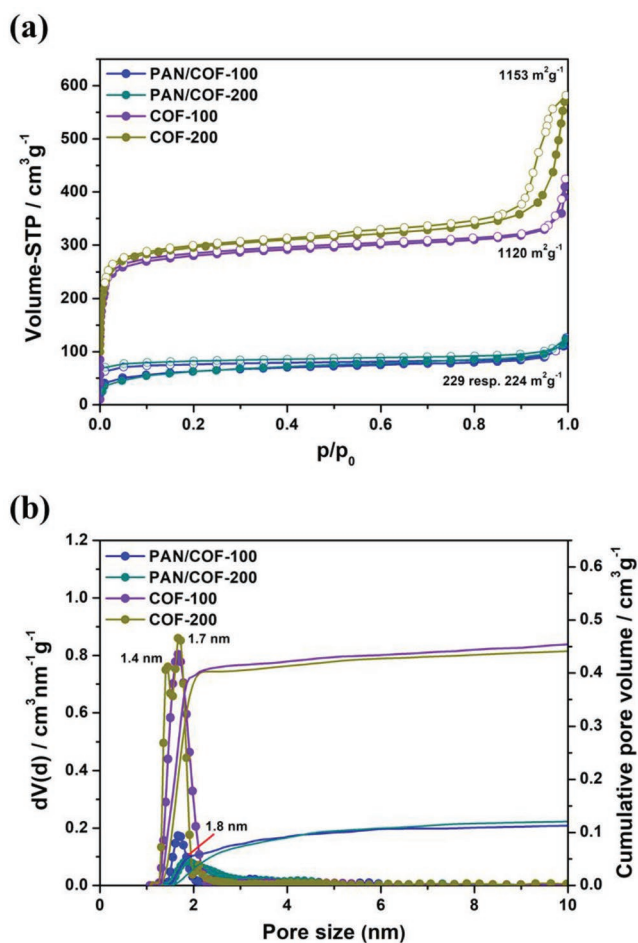


Figure 4. a) N_2 adsorption–desorption isotherms of PAN/COF-100, PAN/COF-200, COF-100, and COF-200, b) their pore size distribution, and cumulative pore volume obtained using the quenched solid density functional theory method.

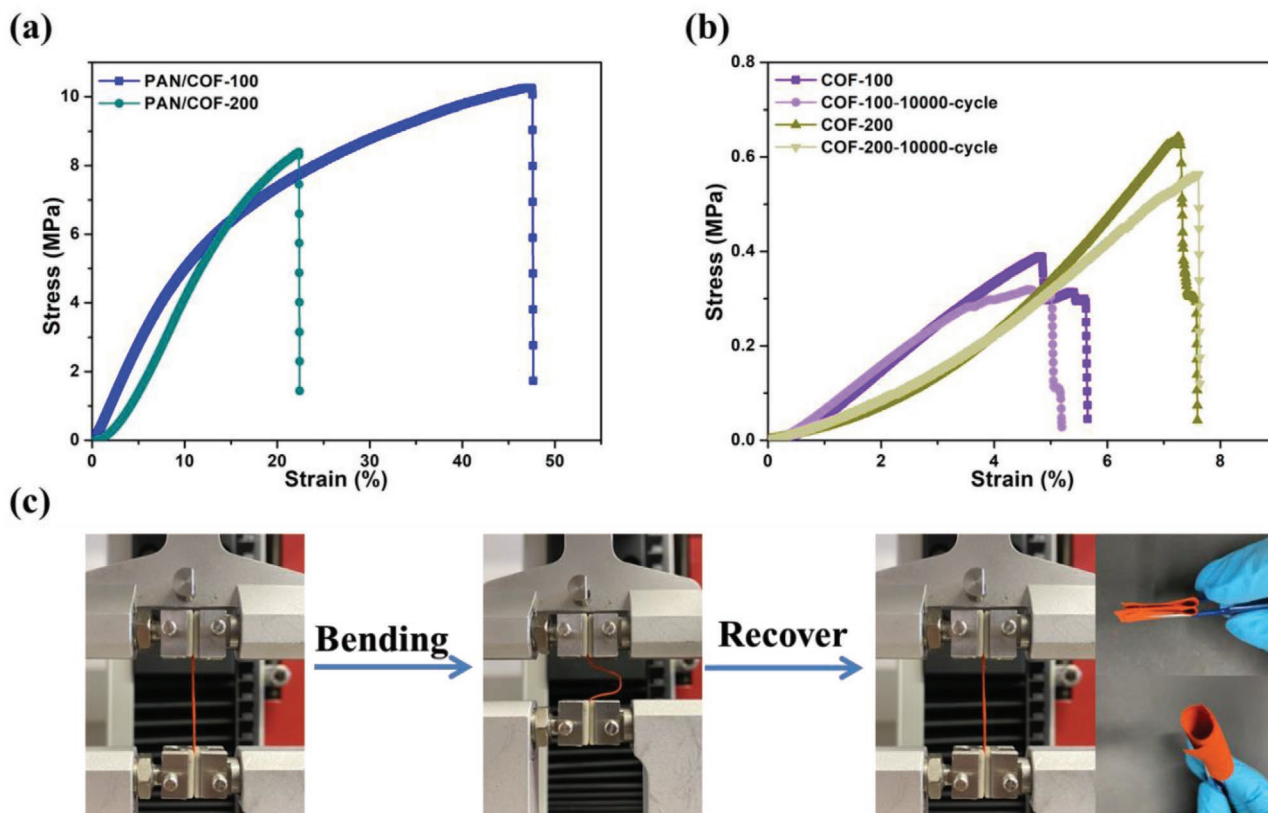


Figure 5. a) Typical stress–strain curves of PAN/COF-100, PAN/COF-200 and b) COF-100, COF-200, and porous COF fiber membranes after 10 000 cycles of bending. c) Bending and recovery processes for the COF, and the test at different bending states.

91.2 ± 6 MPa is reported for sulfonic acid-functionalized COF membranes prepared by self-assembling COF nanosheets.^[23]

To characterize the flexibility of the porous COF fiber membranes, we performed a 10 000 cycle bending test with a compression of 50% and showed the flexibility of the porous COF fiber membranes under different bending states (folding and curling), as shown in Figure 5c. Also, the tensile test showed that the mechanical properties of the porous COF fiber membranes remained basically unchanged, as shown in Figure 5b. Additionally, the sample that underwent a bending cycle did not show any cracks as seen by SEM images, confirming the excellent flexibility and bending stability of porous COF fiber membranes (Figure S7, Supporting Information).

3. Conclusions

The TAF preparation method is successfully established, exemplary for the synthesis of a flexible porous COF membranes with a high specific surface area. The resulting COF membranes were produced in large dimensions, good crystallinity, and excellent hierarchical porosity. In addition, porous COF fiber membranes also show good mechanical stability and outstanding flexibility. After 10 000 cycle bending tests, its mechanical properties are unchanged. The present procedure could be used in the future for making COFs with other organic linkages. The only condition for transferring the current approach

to other COFs is that one of the monomers (starting component) needs to be preloaded on the template polymer fiber. The versatility of the electrospinning procedure allows for preloading during fiber formation by mixing different components either in the form of molecular solution or dispersions in a simple way, making the present procedure very promising.

At the same time, the porous COF fiber membranes also has excellent thermal stability. Therefore, the porous COF fiber membranes and their derivatives have great application prospects in the fields of separation, catalysis, and energy. It is worth mentioning that here prepared membranes are different from the conventional barrier membranes. Our membranes show a hierarchical porosity providing very little resistance for gas mixtures to pass through. Their use within pressure swing or temperature swing adsorption will be beneficial. The macropores allow for an easy gas flow and small pressure drops, at the same time, the ultramicroporosity ensures a good gas uptake and separation. Compared to the often used particle fillings with their problems of compacting, the here prepared membranes can be rolled and thus easily packed into the columns.

4. Experimental Section

Materials: PAN (Mw = 80 000, Carl Roth), Pa, and Tp were purchased from Sigma-Aldrich. DMF (99.9%), dichloromethane (CH₂Cl₂, 99.9%),

and acetic acid (AcOH, 99.7%) were purchased from Fisher Chemical. All chemicals can be used directly without further purification.

Preparation of the Porous COF Fiber Membranes: The porous COF fiber membranes were prepared in three steps. The preparation process is shown in Figure 1. In the first step, PAN/Pa fiber membranes were prepared by electrospinning. 1.5 g of PAN and a certain amount of Pa (1.5 and 3.0 g, respectively) were dissolved in 8.5 g of DMF and stirred for 3 h to form a uniformly dispersed PAN/Pa electrospinning solution. The working voltage, the tip-to-collector distance, and the flow rate were set at 15 kV, 25 cm, and 0.8 mL h⁻¹, respectively. The PAN/Pa fiber membranes with different loading ratios of Pa (100% and 200%) were prepared, which were called PAN/Pa-100 and PAN/Pa-200, respectively. All the prepared PAN/Pa fiber membranes were vacuum dried at room temperature for 12 h. In the second step, PAN/COF fiber membranes were prepared by in situ growth. Take PAN/Pa-200 as an example. The PAN/Pa-200 fiber membrane (100 mg) was added to a dichloromethane (43.2 g) solution containing Tp (86.4 mg) and acetic acid (0.86 g) and reacted at 120 °C for 1 day to obtain red PAN/COF fiber membranes. Then it was washed three times with dichloromethane and acetone, and dried under vacuum at 60 °C for 12 h. The prepared membranes were named PAN/COF-100 and PAN/COF-200, respectively. In the third step, the PAN/COF fiber membranes were washed at 160 °C for 1 day using a Soxhlet extractor and DMF to completely remove PAN and obtain porous COF fiber membranes and dried under vacuum at 60 °C for 12 h. The prepared membranes were named COF-100 and COF-200, respectively. And, the thickness of the porous COF fiber membranes can be easily changed by using electrospun template polymer membranes of different thicknesses, which in turn is controlled by the time of electrospinning keeping all other spinning parameters the same. In addition, PAN fiber membranes and TpPa COF powders were prepared through similar steps for other characterization and testing.

Supporting Information

Supporting Information is available from the Wiley Online Library or from the author.

Conflict of Interest

The authors declare no conflict of interest.

Data Availability Statement

Research data are not shared.

Keywords

covalent organic frameworks, electrospinning, porosity

Received: July 6, 2021

Revised: August 16, 2021

Published online: September 3, 2021

- [1] a) A. P. Cote, A. I. Benin, N. W. Ockwig, M. O’Keeffe, A. J. Matzger, O. M. Yaghi, *Science* **2005**, *310*, 1166; b) N. Huang, P. Wang, D. Jiang, *Nat. Rev. Mater.* **2016**, *1*, 16068; c) C. S. Diercks, O. M. Yaghi, *Science* **2017**, *355*, eaal1585; d) M. S. Lohse, T. Bein, *Adv. Funct. Mater.* **2018**, *28*, 1705553.

- [2] Y. Zeng, R. Zou, Y. Zhao, *Adv. Mater.* **2016**, *28*, 2855.
 [3] a) H. Fan, A. Mundstock, A. Feldhoff, A. Knebel, J. Gu, H. Meng, J. R. Caro, *J. Am. Chem. Soc.* **2018**, *140*, 10094; b) S. Yuan, X. Li, J. Zhu, G. Zhang, P. Van Puyvelde, B. Van der Bruggen, *Chem. Soc. Rev.* **2019**, *48*, 2665.
 [4] a) S. He, B. Yin, H. Niu, Y. Cai, *Appl. Catal. B* **2018**, *239*, 147; b) H. Xu, J. Gao, D. Jiang, *Nat. Chem.* **2015**, *7*, 905.
 [5] a) H. Yang, L. Yang, H. Wang, Z. Xu, Y. Zhao, Y. Luo, N. Nasir, Y. Song, H. Wu, F. Pan, *Nat. Commun.* **2019**, *10*, 2101; b) K. Dey, S. Kunjattu H, A. M. Chahande, R. Banerjee, *Angew. Chem., Int. Ed.* **2020**, *132*, 1177.
 [6] K. Dey, M. Pal, K. C. Rout, S. Kunjattu H, A. Das, R. Mukherjee, U. K. Kharul, R. Banerjee, *J. Am. Chem. Soc.* **2017**, *139*, 13083.
 [7] a) Y. Yusran, H. Li, X. Guan, D. Li, L. Tang, M. Xue, Z. Zhuang, Y. Yan, V. Valtchev, S. Qiu, *Adv. Mater.* **2020**, *32*, 1907289; b) J. Li, X. Jing, Q. Li, S. Li, X. Gao, X. Feng, B. Wang, *Chem. Soc. Rev.* **2020**, *49*, 3565.
 [8] X. Li, Q. Gao, J. Wang, Y. Chen, Z.-H. Chen, H.-S. Xu, W. Tang, K. Leng, G.-H. Ning, J. Wu, *Nat. Commun.* **2018**, *9*, 2335.
 [9] S. Kandambeth, B. P. Biswal, H. D. Chaudhari, K. C. Rout, S. Kunjattu H, S. Mitra, S. Karak, A. Das, R. Mukherjee, U. K. Kharul, *Adv. Mater.* **2017**, *29*, 1603945.
 [10] P. Pachfule, S. Kandambeth, A. Mallick, R. Banerjee, *Chem. Commun.* **2015**, *51*, 11717.
 [11] Y. Peng, M. Zhao, B. Chen, Z. Zhang, Y. Huang, F. Dai, Z. Lai, X. Cui, C. Tan, H. Zhang, *Adv. Mater.* **2018**, *30*, 1705454.
 [12] a) H. S. Sasmal, H. B. Aiyappa, S. N. Bhanage, S. Karak, A. Halder, S. Kurungot, R. Banerjee, *Angew. Chem., Int. Ed.* **2018**, *130*, 11060; b) M. Matsumoto, L. Valentino, G. M. Stiehl, H. B. Balch, A. R. Corcos, F. Wang, D. C. Ralph, B. J. Mariñas, W. R. Dichtel, *Chem* **2018**, *4*, 308.
 [13] a) A. K. Mohammed, S. Usgaonkar, F. Kanheerampockil, S. Karak, A. Halder, M. Tharkar, M. Addicoat, T. G. Ajithkumar, R. Banerjee, *J. Am. Chem. Soc.* **2020**, *142*, 8252; b) C. Li, J. Yang, P. Pachfule, S. Li, M.-Y. Ye, J. Schmidt, A. Thomas, *Nat. Commun.* **2020**, *11*, 4712.
 [14] H. Fan, J. Gu, H. Meng, A. Knebel, J. Caro, *Angew. Chem., Int. Ed.* **2018**, *57*, 4083.
 [15] a) S. Chandra, S. Kandambeth, B. P. Biswal, B. Lukose, S. M. Kunjir, M. Chaudhary, R. Babarao, T. Heine, R. Banerjee, *J. Am. Chem. Soc.* **2013**, *135*, 17853; b) D. W. Burke, C. Sun, I. Castano, N. C. Flanders, A. M. Evans, E. Vitaku, D. C. McLeod, R. H. Lambeth, L. X. Chen, N. C. Gianneschi, *Angew. Chem., Int. Ed.* **2020**, *59*, 5165.
 [16] W. Zhang, L. Zhang, H. Zhao, B. Li, H. Ma, *J. Mater. Chem. A* **2018**, *6*, 13331.
 [17] a) S. Agarwal, A. Greiner, J. H. Wendorff, *Adv. Funct. Mater.* **2009**, *19*, 2863; b) S. Jiang, Y. Chen, G. Duan, C. Mei, A. Greiner, S. Agarwal, *Polym. Chem.* **2018**, *9*, 2685; c) X. Yang, J. Wang, H. Guo, L. Liu, W. Xu, G. Duan, *e-Polymers* **2020**, *20*, 682.
 [18] a) Y. Han, Q. Zhang, N. Hu, X. Zhang, Y. Mai, J. Liu, X. Hua, H. Wei, *Chin. Chem. Lett.* **2017**, *28*, 2269; b) H. Hou, J. J. Ge, J. Zeng, Q. Li, D. H. Reneker, A. Greiner, S. Z. Cheng, *Chem. Mater.* **2005**, *17*, 967.
 [19] S. Kandambeth, A. Mallick, B. Lukose, M. V. Mane, T. Heine, R. Banerjee, *J. Am. Chem. Soc.* **2012**, *134*, 19524.
 [20] a) K. E. Hart, J. M. Springmeier, N. B. McKeown, C. M. Colina, *Phys. Chem. Chem. Phys.* **2013**, *15*, 20161; b) J. Weber, N. Du, M. D. Guiver, *Macromolecules* **2011**, *44*, 1763.
 [21] M. Thommes, K. Kaneko, A. V. Neimark, J. P. Olivier, F. Rodriguez-Reinoso, J. Rouquerol, K. S. Sing, *Pure Appl. Chem.* **2015**, *87*, 1051.
 [22] Z. Wang, Q. Yu, Y. Huang, H. An, Y. Zhao, Y. Feng, X. Li, X. Shi, J. Liang, F. Pan, *ACS Cent. Sci.* **2019**, *5*, 1352.
 [23] L. Cao, H. Wu, Y. Cao, C. Fan, R. Zhao, X. He, P. Yang, B. Shi, X. You, Z. Jiang, *Adv. Mater.* **2020**, *32*, 2005565.